Journal of Molecular Structure 1006 (2011) 600–605

Contents lists available at SciVerse ScienceDirect

Journal of Molecular Structure

journal homepage: www.elsevier.com/locate/molstruc

Factors determining tautomeric equilibria in Schiff bases

Martha Flores-Leonar, Nuria Esturau-Escofet, José M. Méndez-Stivalet, Armando Marín-Becerra, Carlos Amador-Bedolla *

Facultad de Química, Universidad Nacional Autónoma de México, México DF 04510, Mexico

ARTICLE INFO

Article history:
Received 10 August 2011
Received in revised form 12 September 2011
Accepted 8 October 2011
Available online 19 October 2011

Keywords:
Schiff bases
Enol–keto tautomer equilibrium
DFT–GIAO NMR chemical shifts

ABSTRACT

Schiff bases derived from o-hydroxyaldehydes present keto and enol tautomeric forms; the relative equilibrium between these two tautomers depending on the particular aldehyde the Schiff bases is derived from. Thus benzaldehyde produces a stable enol tautomer, while a naphthaldehyde produces a mixture of keto and enol tautomers. The energy difference between these tautomers is very small (~5 kJ/mol) and therefore close to current precision limits of *ab initio* and DFT based quantum calculations. NMR spectroscopy results, which allows for the determination of the stable structure when one tautomer is prevalent, can be very difficult to interpret when both tautomers are present. We calculate energy differences between the tautomers and demonstrate that the precision of current DFT calculations is not sufficient to predict the most stable structure. On the other hand, DFT calculations of the NMR chemical shifts (using the GIAO technique) can properly interpret the spectroscopy results allowing the characterization of the experimentally present tautomers and the estimation of the relative abundance of each when both are present.

1. Introduction

Schiff bases are compounds in which an imine group (—C═N—) is present. Some of them, of the general type $R'C_6H_3(OH)(CH{=}NR'')$, present enol–keto tautomerism. These compounds are synthesized from carbonylic derivatives such as salicylaldehyde or o-hydroxyaldehydes with a monoamine in 1:1 proportion via a single step condensation. These type of compounds have been widely used in biochemistry, coordination chemistry, catalytic reactions and organic synthesis [1–5].

Tautomeric forms enol–imine and keto–amine exist, both presenting an intramolecular hydrogen bond [4–8]. In the solid state both forms have been reported, whereas in solution, salicylaldimines species produce preferently the enol–imine tautomer (enol) while 2-hydroxy-1-naphthaldimines species produce mainly the keto–amine tautomer (keto). Both tautomers have been detected by X-ray structural analyses that show that the transformation from enol–imine to keto–amine is accompanied by a considerable increase in the C—N distance from 1.317 Å to 1.330 Å, as well as the reduction in the C—O distance from 1.279 Å to 1.263 Å [7]. Based on these results it has been proposed that the dominant tautomer depends on the type of carbonylic precursor and not on the stereochemistry of the molecule nor the substituent of the nitrogen of the imine [6,8]. ^{13}C NMR has been widely used for identification of the dominant tautomer, leading to the prediction of a lower limit for the chemical shift of the carbon atom forming an enol bond of 155 ppm, and an upper limit for the keto bond of 180 ppm [9,10].

Equilibrium between the tautomeric forms has been studied also for acidic and basic solutions. Its displacement from the keto–amine tautomer at neutral pH to the enol–imine tautomer at acidic solution being explained in terms of the formation of a hydrogen bond with the acid molecule [7]. However, our ^{1}H and ^{13}C NMR data show that the equilibrium is not displaced to the enol tautomer but instead tautomers are hydrolyzed back to the aldehyde precursor.

In order to further understand this behavior, quantum chemistry calculations were performed for a series of Schiff bases species to compare the stability of the keto and enol forms for different R′ and R″ substituents. Additionally, four of these substances were synthesized and their structure determined by ^{1}H NMR and ^{13}C NMR. We selected 12 different compounds based either on the salicylaldehyde or the naphthaldehyde precursor. According to the usual organic chemistry argument, preservation of aromaticity accounts for the stabilization of the keto tautomer instead of the enol one. We studied this hypothesis by choosing molecules based on the naphthaldehyde precursor both with aromatic rings (based on 2-hydroxy-1-naphthaldehyde and 1-hydroxy-2-naphthaldehyde) and without aromaticity (based on 3-hydroxy-2-naphthaldehyde).

The total of 12 different molecules for studying the enol–keto energy difference is shown in Scheme 1. Molecules **a**, **b**, **c**, and **d** were synthesized and characterized. Notice that molecules **b**, **d**, **f**, **h**, **j**, and **l** preserve some aromaticity in the keto form.

* Corresponding author. Tel.: +52 55 56223804; fax: +52 55 56223776.
E-mail address: carlos.amador@unam.mx (C. Amador-Bedolla).

0022-2860/$ - see front matter © 2011 Elsevier B.V. All rights reserved.
doi:10.1016/j.molstruc.2011.10.011

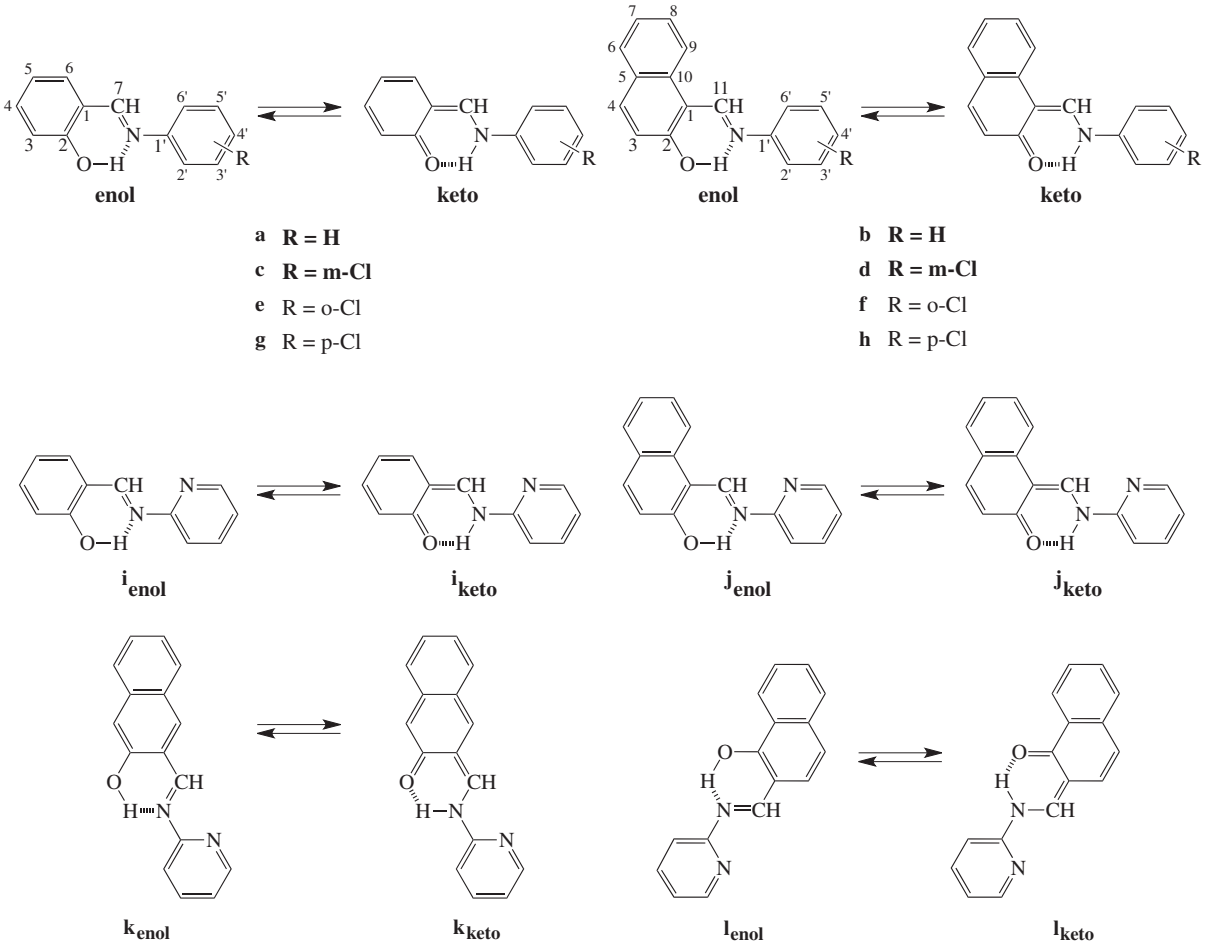

Scheme 1. The 12 different molecules considered in the study of the enol–keto equilibrium.

The rest of this paper is organized as follows. In Section 2 we discuss our quantum chemical calculations and their results. In Section 3 we present our experimental results from ^{1}H NMR and ^{13}C NMR for molecules **a**, **b**, **c**, and **d**. In Section 4 we present results from the GIAO based NMR calculations and use them to interpret experimental results obtained for the four molecules synthesized and predict them for the rest of the molecules. Section 5 show our conclusions.

2. DFT calculations

Density functional theory calculations, using the B3LYP [11,12] functional, were performed for 12 different species both of the keto–amine and enol–imine tautomers. Calculations were carried out using the Gaussian 09W [13] package and employing basis functions of the 6-311++G(d,p) type for all atoms. Optimal geometric structures were obtained for each isolated molecule (gas phase) and also for the molecule in solution using the Polarizable Continuum Model (PCM). Solvents used for NMR spectra of **a**, **b**, **c**, and **d**, $CHCl_3$ and DMSO, were considered.

Table 1 shows the energy differences between enol and keto tautomers.

Results show that for species based on benzaldehyde (**a**, **c**, **e**, **g**, and **i**) the enol–imine form is favored strongly in gas phase, while for species based in either 1-2 or 2-1-naphthaldehyde the energy difference between enol–imine and keto–amine is small, justifying the possibility of both tautomers being observed at room temperature. Only two species (**j** and **l**) favored the keto–amine tautomer in the gas phase. The solvent effect reduce the difference between the enol and the keto form and favors stability of the latter. In DMSO this stabilization is large averaging more than 10 kJ/mol, thus turning the slightly favorable enol tautomer into a slightly favorable keto tautomer for all species based in naphthaldehyde. Still, this change in energy difference, resulting in a more stable keto tautomer by −5.2 kJ/mol in the case of species **d** for example, is in the limit of precision of DFT calculations. Whether the observed structure corresponds to the keto form can not be

Table 1
Energy differences between the enol–imine and keto–amine tautomers for the 12 species considered, $\Delta E = E_{keto} - E_{enol}$, in kJ/mol. The presence of a solvent is modeled with PCM for $CHCl_3$ and DMSO.

Species	6-311++G(d,p) PCM		
	Gas	$CHCl_3$	DMSO
a	+19.5	+10.9	+6.9
b	+2.4	−4.3	−7.3
c	+21.8	+13.5	+9.7
d	+4.3	−2.2	−5.2
e	+21.3	+16.0	+11.9
f	+6.3	−0.4	−3.4
g	+20.2	+13.1	+9.1
h	+4.3	−2.4	−5.5
i	+14.2	+6.9	+3.8
j	−3.2	−8.7	−10.9
k	+32.8	+23.4	+19.2
l	−7.1	−12.0	−14.1

predicted based on this energy difference. At most, these results can be used to predict that, in DMSO, most molecules based on benzaldehyde will be present in the enol form, with the possible exception of molecules **a** and **i** that can present a mixture of the two tautomers at room temperature. Correspondingly, species based on naphthaldehyde will favor either the existence of a mixture of the enol and keto tautomers for species **d**, **f**, and **h** or perhaps only the keto form for species **b**, **j**, and **l**. In $CHCl_3$, the stabilization of the keto tautomer is less pronounced, averaging 7 kJ/mol. This is reflected in the experimental results on species **b** and **d**, which show a higher proportion of the keto tautomer in the estimated equilibrium constant for DMSO (see below Section 4).

This predictions could be confirmed by synthesizing the actual compounds. As mentioned earlier, we were able to synthesize species **a** and **c** (benzaldehyde based, enol favoring) and **b** and **d** (naphthaldehyde based, mixed tautomers favoring). NMR spectra were obtained for these four species (see below) and their structure analyzed with the help of calculated chemical shifts for C atoms as obtained by the use of the GIAO method [14] available through the calculation performed by using the Gaussian 09W [13] package.

In addition, results from the calculations were used to rationalize how the electronic structures (HOMO, LUMO energies and their distribution in the molecule) of enol and keto tautomers differ, and how these differences change when the species is based on benzaldehyde with respect to when it is based on naphthaldehyde.

3. Experimental and NMR results

All solvents and reagents were used as received. ^1H and ^{13}C NMR spectra were determined using a Varian VNMR-400 MHz spectrometer (399.96 MHz for ^1H and 100.58 MHz for ^{13}C) at 299 K. Chemical shifts (δ in ppm) are referenced to solvent peaks $CDCl_3$ 7.26 for ^1H and 77.0 for ^{13}C, DMSO-d_6 2.49 for ^1H and 39.5 for ^{13}C.

Both one-dimensional (^1H and ^{13}C) and two-dimensional 2D NMR (inverse detected HSQC and HMBC) spectra were acquired with standard conditions and with standard pulse programs taken from the Varian software library.

3.1. Synthesis of (E)-2-((phenylimino)methyl)phenol (Scheme 1a)

To a solution of salicylaldehyde (500 μL, 4.7 mmol) in methanol (50 mL), a solution of aniline (428 μL, 4.7 mmol) in methanol (10 mL) was added while stirring. The reaction mixture was stirred for additional 30 min. The volume was then reduced in half and the solution cooled at −18 °C for a couple of hours. A yellow crystalline solid was obtained which was filtered off under vacuum and washed with 20 mL of cold ether. Yield 0.6489 g (70.2%).

3.2. Synthesis of (E)-1-((phenylimino)methyl)naphthalen-2-ol and (Z)-1-((phenylamino)methylene)naphthalen-2-one (Scheme 1b)

To a solution of 2-hydroxy-1-naphthaldehyde (0.5 g, 2.9 mmol) in methanol (50 mL), a solution of aniline (264 μL, 2.9 mmol) in methanol (10 mL) was added while stirring. The reaction mixture was stirred for additional 30 min. The volume was then reduced *in vacuo* to 20 mL and the resulting solution was cooled at −18 °C for a couple of hours. On cooling, a yellow crystalline solid was obtained which was filtered off, washed with 20 mL of cold ether and dried under vacuum. Yield 0.6675 g (93.4%).

3.3. Synthesis of (E)-2-((3-chlorophenylimino)methyl)phenol (Scheme 1c)

To a solution of salicylaldehyde (500 μL, 4.7 mmol) in methanol (50 mL), a solution of m-chloroaniline (496 μL, 4.7 mmol) in methanol (10 mL) was added while stirring. The reaction mixture was stirred for additional 30 min. The volume was then reduced in half and the solution cooled at −18 °C for a couple of hours. A yellow crystalline solid was obtained which was filtered off under vacuum and washed with 20 mL of cold ether. Yield 1.0152 g (93.5%).

3.4. Synthesis of (E)-1-((3-chlorophenylimino)methyl)naphthalen-2-ol and (Z)-1-((3-chlorophenylamino)methylene)naphthalen-2-one (Scheme 1d)

To a solution of 2-hydroxy-1-naphthaldehyde (0.5 g, 2.9 mmol) in methanol (50 mL), a solution of m-chloroaniline (307 μL, 2.9 mmol) in methanol (10 mL) was added while stirring. The reaction mixture was stirred for additional 30 min. The volume was then reduced *in vacuo* to 20 mL and the resulting solution was cooled at −18 °C for a couple of hours. On cooling, a yellow crystaline solid was obtained which was filtered off, washed with 20 mL of cold ether and dried under vacuum. Yield 0.5733 g (70.2%).

^1H and ^{13}C NMR results for **a**(**c**) show that the enol tautomer is obtained exclusively without presence of keto tautomer. For ^1H NMR in $CDCl_3$ the OH proton is observed at 13.3(12.9) ppm as a broad signal, while the proton joined to the Schiff base carbon atom (N═CH—Ar) appears as a singlet at 8.6(8.6) ppm. The aromatic protons appear from 6.9 to 7.5(6.9 to 7.5) ppm. ^1H NMR in DMSO results show similar shifts with the OH proton appearing at 13.1(12.7) ppm also as a broad signal, the N═CH—Ar proton is now observed at 8.9(8.9) ppm and the aromatic signals appear from 6.9 to 7.7(6.9 to 7.7) ppm.

In contrast, when the precursor is 2-hydroxy-1-naphthaldehyde, structure **b**(**d**), ^1H NMR studies show that tautomeric equilibria is present in both $CDCl_3$ and DMSO. In $CDCl_3$ the NH proton is observed at 15.5(15.1) ppm as a doublet (J = 4.7(2.7) Hz), and the proton corresponding to the Schiff base carbon (N—CH═Ar) is observed also as a doublet at 9.3(9.3) ppm (J = 4.7(2.7) Hz); these results are only possible for a keto–amine form owing to the location of the hydrogen atom on nitrogen. The presence of this doublet deserves special comment. In a slow regime we would observe two signals, corresponding to both keto and enol tautomers, a singlet for enol and a doublet for keto, the latter due to the —HN—CH═coupling. However, since the equilibrium between ceto and enol tautomers is a very fast interconversion, we observe an averaged signal from the doublet and the singlet, *i.e.* a pseudo-doublet without a well defined minimum (see Supplementary information). This coupling has been observed in similar systems with coupling constant, $^3J_{HNCH}$, values in the range 2–4 Hz [15]. To confirm this assertion, we also measured ^1H NMR signals at lower temperatures for species **b** in $CDCl_3$ and found that, at −20 °C, the doublet shifts high field, the coupling constant increases from 4.0 Hz to 6.0 Hz, and the minimum is now well defined; moreover, at −50 °C, the doublet shifts to high field even more, the coupling constant increases further to 7.2 Hz and the minimum is even more pronounced (see Supplementary information). Thus, at lower temperatures the equilibrium is shifted even more towards the stable keto form, in agreement with calculations (see Section 2).

Aromatic protons appear from 7.0 to 8.1(7.1 to 8.1) ppm. For structure **d**, the minor peaks appearing as singlets at 13.1 ppm for OH proton and at 10.8 ppm for the H—(C═O)—Ar proton are attributed to the hydrolyzed compound, which was detected by HMBC experiment observing a correlation at 193 ppm for ^{13}C

which corresponds to the aldehyde carbon atom displacement of the 2-hydroxy-1-naphthaldehyde precursor.

When solvent is changed to DMSO, for structure **b**(**d**), signals corresponding to NH and N—CH=Ar groups are found as singlets at 15.8(15.5) and 9.6(9.7) ppm respectively, this is due to the solvent coordinating to the acidic proton involved in the equilibrium, thus eliminating the posibility of coupling between these two protons. The aromatic protons signals appear from 7.0 to 8.5 ppm.

In ^{13}C NMR, the principal differences between the structures **a**(**c**) and **b**(**d**) can be observed on carbon 2 and on Schiff base carbon (atom 7 in **a**, **c** and 11 in **b**, **d**). For structure **a**(**c**), the chemical shifts in $CDCl_3$ are 161.11(161.13) ppm and 162.64(163.68) ppm for C2 and C7 respectively, while in DMSO are 160.26(160.19) and 163.49(164.69) ppm; *i.e.* C2 (enol carbon) is upfield from the Schiff base carbon C7. When the precursor is changed to 2-hydroxy-1-naphthaldehyde, **b**(**d**), ^{13}C NMR chemical shifts change, displacing significantly the C2 signal downfield at 171.23(168.28) ppm, thus inverting Schiff base carbon (now C11) which appears at 154.15(156.43) ppm in $CDCl_3$; a similar thing happens in DMSO where shift values are 171.16(169.01) and 155.25(157.08) ppm. This change implies the presence of the keto–amine tautomer, and therefore, tautomeric equilibrium.

4. GIAO calculation and interpretation

Gauge Invariant Atomic Orbitals (GIAO) basis set allows the theoretical prediction of chemical displacements through the calculation of magnetic shielding tensors [14]. The best "virtual" reference standard needed for this calculation has been the subject of recent studies [16,17]. According to Sarotti and Pellegrinet [17], a good selection for sp^2 ^{13}C in DFT calculations as a reference standard is benzene. The predicted chemical shift for a given nucleus (δ^x_{calc}) is calculated as

$$\delta^x_{calc} = \sigma_{ben} - \sigma_x + \delta_{ben}, \quad (1)$$

where σ_{ben} and σ_x are the NMR isotropic magnetic shielding values for benzene and the corresponding nucleus, respectively, and δ_{ben} is the experimental chemical shift of benzene (128.62 ppm in benzene, 128.37 ppm in $CDCl_3$, and 128.30 ppm in DMSO [18]).

For species **a** and **c**, calculated chemical shifts for a given ^{13}C atom differ only slightly (less than 7 ppm) between enol and keto tautomers, except for atoms $C_2, C_7, C_{1'}, C_3$ (Scheme 1 **a** and **c**). Table 2 shows calculated chemical shifts for these atoms both for enol and keto tautomers, as well as measured chemical shifts for the synthesized compounds. For species **a** enol calculated and experimental values have a MAD of 2.29 (2.94) ppm, while keto calculated and experimental values have a MAD of 13.70 (14.32) ppm in $CDCl_3$ (DMSO); while for species **c** enol calculated and experimental values have a MAD of 2.37 (2.75) ppm, while keto calculated and experimental values have a MAD of 14.45 (15.18) ppm in $CDCl_3$ (DMSO). The correspondence between the experimental values and the enol tautomer confirms the experimental interpretation that this is the structure present in solution both for $CDCl_3$ and DMSO.

For species **b** and **d**, differences between calculated chemical shifts for the enol and keto tautomers are substantial only for the same set of four carbon atoms as in species **a** and **c**, $C_2, C_{11}, C_{1'}, C_3$ (Scheme 1 **b** and **d**). Table 3 shows calculated chemical shifts for these atoms both for enol and keto tautomers, as well as measured chemical shifts for the synthesized compounds. For species **b**, enol calculated and experimental values have a MAD of 4.73 (4.44) ppm, while keto calculated and experimental values have a MAD of 9.81 (9.92) ppm in $CDCl_3$ (DMSO); that is, an increase in MAD for the enol tautomer and a decrease for the keto tautomer with respect to values for species **a**. Similarly, for species **d**, enol calculated and experimental values have a MAD of 3.02 (3.85) ppm, while keto calculated and experimental values have a MAD of 11.41 (10.99) ppm in $CDCl_3$ (DMSO); showing also an increase in MAD for the enol tautomer and a decrease for the keto tautomer with respect to values for species **c**. Moreover, while

Table 2
Chemical shifts (ppm) of selected atoms for species **a** and **c**. Experimental and calculated (both enol and keto tautomers) in $CDCl_3$ and DMSO. Calculated isotropic magnetic shielding values for benzene used in Eq. (1) are 49.55 and 49.45 for $CDCl_3$ and DMSO, respectively.

	Atom	$CDCl_3$				DMSO			
		δ_{exp}	δ_{enol}	δ_{keto}	$\delta_{enol} - \delta_{keto}$	δ_{exp}	δ_{enol}	δ_{keto}	$\delta_{enol} - \delta_{keto}$
a	C_2	161.11	166.02	184.24	−18.23	160.26	166.02	184.41	−18.39
	C_7	162.64	162.47	147.76	+14.71	163.49	162.03	147.50	+14.53
	$C_{1'}$	148.48	152.33	140.71	+11.62	148.06	151.87	140.44	+11.43
	C_3	117.22	117.43	126.22	−8.79	116.57	117.31	126.09	−8.79
c	C_2	161.13	166.34	184.21	−17.87	160.19	166.35	184.34	−17.99
	C_7	163.68	164.16	146.56	+17.60	164.69	163.88	146.56	+17.32
	$C_{1'}$	149.83	153.42	141.58	+11.83	149.86	153.10	141.41	+11.69
	C_3	117.33	117.54	126.70	−9.15	116.61	117.39	126.59	−9.19

Table 3
Chemical shifts (ppm) of selected atoms for species **b** and **d**. Experimental and calculated (both enol and keto tautomers) in $CDCl_3$ and DMSO. Calculated isotropic magnetic shielding values for benzene used in Eq. (1) are 49.55 and 49.45 for $CDCl_3$ and DMSO, respectively.

	Atom	$CDCl_3$				DMSO			
		δ_{exp}	δ_{enol}	δ_{keto}	$\delta_{enol} - \delta_{keto}$	δ_{exp}	δ_{enol}	δ_{keto}	$\delta_{enol} - \delta_{keto}$
b	C_2	171.23	167.35	185.91	−18.57	171.16	167.39	186.12	−18.73
	C_{11}	154.15	158.11	139.10	+19.00	155.25	157.61	139.09	+18.52
	$C_{1'}$	144.75	152.67	141.14	+11.53	143.60	152.15	140.98	+11.17
	C_3	122.54	119.40	128.45	−9.05	122.39	119.30	128.32	−9.02
d	C_2	168.28	167.57	186.23	−18.67	169.01	167.57	186.37	−18.80
	C_{11}	156.43	159.24	140.54	+18.70	157.08	158.82	140.51	+18.32
	$C_{1'}$	147.64	153.99	142.93	+11.06	146.04	155.68	142.78	+12. 90
	C_3	121.37	119.15	128.47	−9.33	121.63	119.04	128.38	−9.34

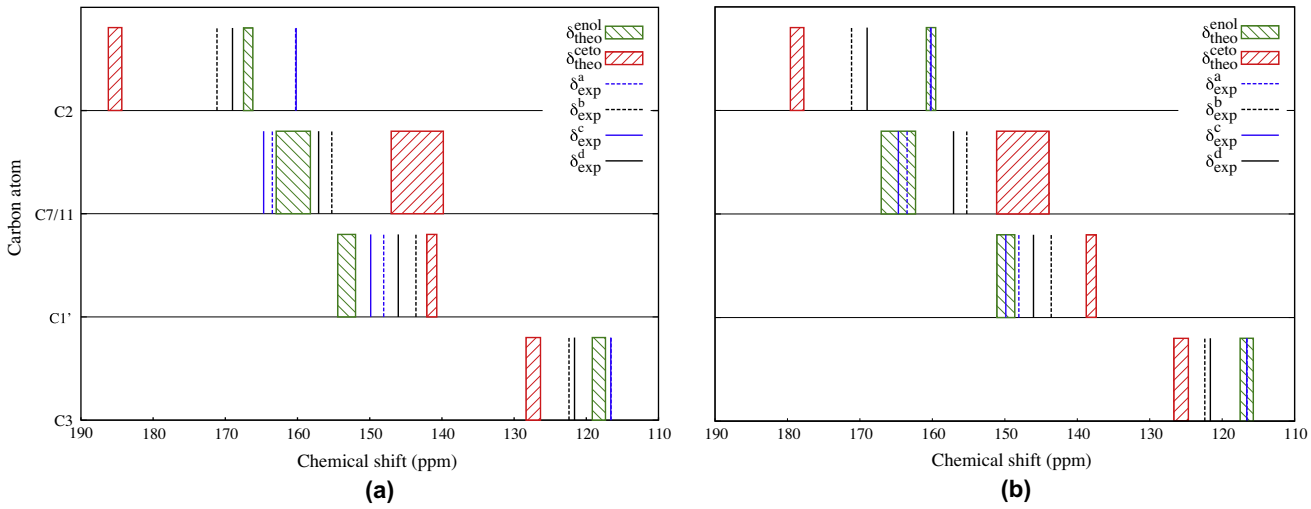

Fig. 1. Chemical shifts for the four carbon atoms that differ the most between the enol and keto tautomers. Green (red) bars correspond to enol (keto) predicted chemical shifts for species **a, b, c, d**. Blue lines correspond to experimental values for species **a** and **c**, while black lines to experimental values for species **b** and **d**. (a) Predicted chemical shifts from DFT/GIAO calculations. In (b) predicted chemical shifts have been displaced by a constant to agree with the experimental value for species **c**. The displacement needed is less than 7 ppm for all four carbon atoms. (For interpretation of the references to color in this figure legend, the reader is referred to the web version of this article.)

for species **a** and **c** experimental values were mostly outside the range between enol and keto predictions, for species **b** and **d** all experimental values are inside this range. This confirms the experimental interpretation (based both on ^{1}H NMR and ^{13}C, see above) that tautomeric equilibrium is present in solution for species **b** and **d**.

Predictions from DFT/GIAO calculations are not exact, although they are precise enough to point to the presence of tautomeric equilibrium for species **b** and **d**, as shown in Fig. 1a. We assume that a constant shift can be used to adjust the calculated chemical shift for species **c**, *i.e.* enol only; and then apply this shift to all other species. All experimental measures for species **b** and **d** lie in the middle of the interval between the chemical shifts corresponding to enol and keto tautomers, as shown in Fig. 1b. We can thus calculate the equilibrium constant,

$$K_{\mathrm{eq}} = \frac{\mathrm{keto}}{\mathrm{enol}} = \frac{1}{4}\sum_{i} \frac{|\delta_i^{\alpha,exp} - \delta_i^{enol,avg}|}{|\delta_i^{keto,avg} - \delta_i^{\alpha,exp}|}, \qquad (2)$$

where $i = \{C_2, C_{7/11}, C_3, C_{1'}\}$, $\delta_i^{\alpha,exp}$ is the experimental value for species α = {**b**,**d**}, and $\delta^{enol(keto),avg}$ is the average of calculated values for enol (keto) species **a, b, c, d**. For species **b** the calculated equilibrium constant corresponds to 53% (58%) keto tautomer present in solution for $CDCl_3$ (DMSO), while for species **d**, corresponds to 36% (45%), in agreement with the total energy calculations that predict a more stable keto tautomer for species **b** than **d** and for solution in DMSO than in $CDCl_3$.

As an example of the precision required for total energy differences to match this prediction of the equilibrium constant we take species **d**. According to a simple Boltzmann distribution of the relative abundance of the keto and enol tautomers at room temperature, based on the energy differences calculated using DFT (Table 1, species **d**), equilibrium constants should correspond to 71% (89%) keto tautomer presence in solution for $CDCl_3$ (DMSO), that is, two times bigger than estimations based on DFT/GIAO adjusted values. To make total energy calculations match DFT/GIAO estimations, the energy difference between keto and enol tautomers should change from −2.2(−5.2) kJ/mol to +1.4 (+0.5) kJ/mol for $CDCl_3$ (DMSO). These changes in energy differences are smaller than current precision of DFT based calculations.

5. Discussion and conclusions

Enol and keto tautomers are very close in energy for Schiff bases and thus compete closely for stability. While the keto form is disfavored by the destruction of the aromatic ring as compared to the enol form, the creation of a more stable O···H—N hydrogen bond (as compared to O—H···N) could be argued in favor of the keto over the enol form. According to the present results both experimental and theoretical, the stability depends only on the existence of aromaticity, even though the polarity of the solvent stabilizes the keto form.

The creation of the keto form always destroy the aromaticity of the nearby phenyl ring. Therefore, the keto form is normally less stable than the enol form. But if a second aromatic ring is present, and the change from enol to keto maintains the aromaticity of this second ring, the keto form will be the stable one. It has been known for a long time that naphthol Schiff bases derivatives (which preserve an aromatic ring in the keto form) can easily react through its keto form, while phenol Schiff bases derivatives are more difficult to react in this way (Bucherer reaction [19]). In naphthol based compounds an aromatic ring is preserved, stabilizing the intermediate species, while in phenol based ones this is not possible. This explanation applies to the equilibria of structures **a**, **c**, **e**, **g**, and **i**, phenol based, for which the enol form is always stable; and to structures **b**, **d**, **f**, **h**, and **l**, naphthol based, for which the keto form is more stable. A special case is structure **k**, which although naphthol based, cannot keep its aromaticity in the keto form an thus favors the enol form.

The definition of an universal parameter that accounts for aromaticity has been sought for extensively but is still lacking [20]. Amongst the numerous parameters suggested, the most used are the nucleus independent chemical shift (NICS) [21], the harmonic oscillator measure of aromaticity (HOMA) [22], and the aromatic stabilization energy [23]; notwithstanding the use of the HOMO–LUMO gap for the estimation of aromaticity [24]. For the estimation of the change in aromaticity between the enol and keto tautomers in our Schiff bases we use the HOMO–LUMO gap obtained from DFT calculations. For species **a**, **c**, **e**, and **g** (phenol based) the average reduction in the HOMO–LUMO gap is 0.0317 Ha (i.e. the reduction in aromaticity) corresponding to a more stable enol form. Whereas for species **b**, **d**, **f**, and **h** (naphthol based) the average reduction in the HOMO–LUMO gap is 0.0142 Ha

corresponding to a much smaller reduction of the aromaticity and thus favoring the stability of the keto form. Accordingly, species **i** and **k** show a reduction of the HOMO–LUMO gap in going from enol to keto forms of 0.0245 Ha and 0.0344 Ha; such large reduction correlates with a more stable enol form. Finally, species **j** and **l** show small reductions of 0.0067 Ha and 0.0096 Ha and also a much stabler keto form.

Schiff bases present a subtle tautomeric equilibria between the enol and keto forms. The energy difference between these tautomers is very close to the precision limit of current quantum mechanical calculations. Even though, theoretical results allow for the prediction of the presence of both tautomers in solution. This prediction has been confirmed by experimental analysis of the synthesized compounds. The use of theoretical estimations of chemical shifts, based on the GIAO method, allows for the interpretation of NMR spectra.

Acknowledgements

C. A.-B. is thankful to DGAPA–UNAM for financial support (PAPIIT IN206507) and to DGTIC–UNAM for supercomputer access. A. M.-B. acknowledges CONACyT through Project 41933-Q.

Appendix A. Supplementary material

Supplementary data associated with this article can be found, in the online version, at doi:10.1016/j.molstruc.2011.10.011.

References

[1] H. Okawa, H. Furutachi, D. Fenton, Coord. Chem. Rev. 174 (1998) 51–75.
[2] N. Youssef, E. El-Zahany, A. El-Seidy, A. Caselli, S. Fantauzzi, S. Cenini, Inorg. Chim. Acta 362 (2009) 2006–2014.
[3] K. Gupta, A. Sutar, Coord. Chem. Rev. 252 (2008) 1420–1450.
[4] M. Yildiz, Z. Kiliç, T. Hökelek, J. Mol. Struct. 441 (1998) 1–10.
[5] T. Hökelek, Z. Kiliç, M. Işiklan, M. Toy, J. Mol. Struct. 523 (2000) 61–69.
[6] R. Hernández-Molina, A. Mederos, Comprehensive Coordination Chemistry II, Pergamon, pp. 411–446.
[7] H. Nazir, M. Yildiz, H. Yilmaz, M. Tahir, D. Ülkü, J. Mol. Struct. 524 (2000) 241–250.
[8] J. Costamagna, J. Vargas, R. Latorre, A. Alvarado, G. Mena, Coord. Chem. Rev. 119 (1992) 67–88.
[9] S.H. Alarcón, A.C. Olivieri, M. González-Sierra, J. Chem. Soc., Perkin Trans. 2 (1994) 1067–1070.
[10] S.H. Alarcón, A.C. Olivieri, D. Sanz, R.M. Claramunt, J. Elguero, J. Mol. Struct. 705 (2004) 1–9.
[11] A. Becke, J. Chem. Phys. 98 (1993) 5648–5652.
[12] C. Lee, W. Yang, R. Parr, Phys. Rev. B 37 (1988) 785–789.
[13] M.J. Frisch, G.W. Trucks, H.B. Schlegel, G.E. Scuseria, M.A. Robb, J.R. Cheeseman, G. Scalmani, V. Barone, B. Mennucci, G.A. Petersson, H. Nakatsuji, M. Caricato, X. Li, H.P. Hratchian, A.F. Izmaylov, J. Bloino, G. Zheng, J.L. Sonnenberg, M. Hada, M. Ehara, K. Toyota, R. Fukuda, J. Hasegawa, M. Ishida, T. Nakajima, Y. Honda, O. Kitao, H. Nakai, T. Vreven, J.J.A. Montgomery, J.E. Peralta, F. Ogliaro, M. Bearpark, J.J. Heyd, E. Brothers, K.N. Kudin, V.N. Staroverov, R. Kobayashi, J. Normand, K. Raghavachari, A. Rendell, J.C. Burant, S.S. Iyengar, J. Tomasi, M. Cossi, N. Rega, J.M. Millam, M. Klene, J.E. Knox, J.B. Cross, V. Bakken, C. Adamo, J. Jaramillo, R. Gomperts, R.E. Stratmann, O. Yazyev, A.J. Austin, R. Cammi, C. Pomelli, J.W. Ochterski, R.L. Martin, K. Morokuma, V.G. Zakrzewski, G.A. Voth, P. Salvador, J.J. Dannenberg, S. Dapprich, A.D. Daniels, O. Farkas, J.B. Foresman, J.V. Ortiz, J. Cioslowski, D.J. Fox, Gaussian 09, Revision A.02, 2009. Gaussian, Inc., Wallingf.
[14] R. Ditchfield, J. Chem. Phys. 56 (1972) 5688–5691.
[15] R. Claramunt, C. López, M.S. María, D. Sanz, J. Elguero, Prog. Nucl. Magn. Reson. Spectrosc. 49 (2006) 169–206.
[16] R. Jain, T. Bally, P.R. Rablen, J. Org. Chem. 74 (2009) 4017–4023.
[17] A. Sarotti, S. Pellegrinet, J. Org. Chem. 74 (2009) 7254–7260.
[18] H.E. Gottlieb, V. Kotlyar, A. Nudelman, J. Org. Chem. 62 (1997) 7512–7515.
[19] H.T. Bucherer, J. Prakt. Chem. 69 (1904) 49–91.
[20] M. Alonso, B. Herradón, J. Comput. Chem. 31 (2010) 917–928.
[21] P. Schleyer, C. Maerker, A. Dransfeld, H. Jiao, N. Hommes, J. Am. Chem. Soc. 118 (1996) 6317–6318.
[22] T. Krygowski, J. Chem. Inf. Comp. Sci. 33 (1993) 70–78.
[23] M. Cyranski, P. Schleyer, T. Krygowski, H. Jiao, G. Hohlneicher, Tetrahedron 59 (2003) 1657–1665.
[24] F. De Proft, P. Geerlings, Chem. Rev. 101 (2001) 1451–1464.